Off-Plane Grazing Incidence Constellation-X Grating Calibrations using Polarized Synchrotron Radiation and PCGRATE Code Calculations

J. F. Seely,[a] L. I. Goray,[b] Benjawan Kjornrattanawanich,[c] J. M. Laming,[a] G. E. Holland,[d]
K. A. Flanagan,[e] R. K. Heilmann,[e] C.-H. Chang,[e] M. L. Schattenburg,[e]
and A. P. Rasmussen[f]

[a]Space Science Division, Naval Research Laboratory, Washington DC 20375
[b]International Intellectual Group Inc., P. O. Box 335, Penfield NY 14526
[c]Universities Space Research Association, National Synchrotron Light Source,
Beamline X24C, Brookhaven National Laboratory, Upton NY 11973
[d]SFA Inc., 2200 Defense Highway, Suite 405, Crofton MD 21114
[e]Kavli Institute for Astrophysics and Space Research, Massachusetts Institute of Technology,
Cambridge MA 02139
[f]Columbia Astrophysical Laboratory, 550 West 120th Street, New York NY 10027

ABSTRACT

Efficiency measurements of a grazing-incidence diffraction grating, planned for the *Constellation-X* Reflection Grating Spectrometer (RGS), were performed using polarized synchrotron radiation at the NRL Brookhaven beamline X24C. The off-plane TM and TE efficiencies of the 5000 groove/mm MIT test grating, patterned on a silicon wafer, were measured and compared to the efficiencies calculated using the PCGRATE-SX code. The calculated and measured efficiencies are in agreement when using groove profiles derived from AFM measurements. The TM and TE efficiencies differ, offering the possibility of performing unique astrophysical science studies by exploiting the polarization sensitivity of the off-plane gratings. The grating calibrations demonstrate the importance of using polarized synchrotron radiation and code calculations for the understanding of the *Constellation-X* grating performance, in particular the effects of the groove profile and microroughness on the efficiency. The optimization of grazing-incidence gratings, for both the off-plane and in-plane mounts, planned for the RGS and x-ray spectrometers on other missions will require detailed synchrotron measurements and code calculations.

Keywords: diffraction grating, soft x-ray-EUV spectroscopy

1. INTRODUCTION

In order to achieve the science objectives for the planned *Constellation-X* mission and other similar x-ray astrophysical missions, high spectral resolution and instrument sensitivity are required in the soft x-ray wavelength range (1 nm to 20 nm). This can only be achieved by grazing incidence diffraction gratings. While the in-plane (classical) grating mount has traditionally been considered for future missions, with the grating grooves perpendicular to the incident beam, it has been recently suggested that the off-plane (conical) grating mount can provide superior performance. The choice of grating mount (in-plane or off-plane) depends on the ability to reliably design, produce, and replicate optimized gratings with high diffraction efficiencies. The accurate experimental measurement of the efficiencies of test gratings, and the validation of efficiency simulation codes, are essential to this process.

Optics for EUV, X-Ray, and Gamma-Ray Astronomy II, edited by Oberto Citterio, Stephen L. O'Dell,
Proc. of SPIE Vol. 5900, 59000B, (2005) · 0277-786X/05/$15 · doi: 10.1117/12.615943

Compared to gratings in the classical in-plane mount, gratings in the off-plane mount have the potential for superior resolution and efficiency.[1-5] The absolute efficiencies in higher orders in grazing off-plane diffraction geometries may reach very high values comparable to those obtained in the first order, which permits using the high orders in the shortest-wavelength part of the operating range to the maximum extent possible.[6] In addition, efficiency calculations indicate off-plane gratings, when properly oriented, can provide polarization sensitivity.[6] The polarization measurements can provide unique information about astrophysical sources not possible with existing instruments such as *XMM-Newton RGS* and *Chandra*, and a grazing incidence off-plane grating has been suggested for the *Constellation-X* mission.[7]

Off-plane grating efficiencies were first measured by Werner[8] using an electron-bombarded anode at four discrete wavelengths in the 0.83 nm to 4.45 nm range. Hunter at NRL measured off-plane and in-plane efficiencies in the 20 nm to 110 nm wavelength range.[9] Off-plane grating measurements using an electron-bombarded x-ray source were carried out in association with a rocket spectrometer mission by Cash *et al.*[5,10,11] More recently, measurements of test gratings were performed by McEntaffer *et al.*[12,13]

Measurements of a test grating, fabricated on a silicon wafer at the MIT Space Nanotechnology Laboratory, were performed at four discrete wavelengths in the 0.99 nm to 4.48 nm range.[14] Measurements of several MIT test gratings were performed in off-plane and in-plane mounts using the ALS synchrotron, in one polarization orientation, by Rasmussen et al.[15]

2. CONICAL DIFFACTION PATTERN

The 5000 groove/mm master grating was fabricated at the MIT Space Nanotechnology Laboratory by use of anisotropic etching of a bias cut silicon wafer.[14] Replica gratings were produced by nanoimprint lithography and were coated with 5 nm of titanium and 20 nm of gold.[16] SEM images of the groove facets indicated a blazed groove profile and low microroughness. The design blaze angle was 7.5°, but as discussed below the efficiency measurements and the PCGRATE-SX code calculations, using the groove profile derived from AFM, indicate that the effective blaze angle after coating was approximately 13° to 15°.

The efficiency calibrations were performed at the NRL beamline X24C at the National Synchrotron Light Source. As shown schematically in Fig. 1, the beamline's monochromator provides dispersed radiation to a large calibration chamber that is a distance of 15 m from the monochromator and 30 m from the synchrotron. The synchrotron radiation from the wiggler magnet is polarized with the electric vector in the plane of the storage ring. The X24C beamline optics, operating at grazing angles in the x-ray and EUV wavelength regions, preserve the polarization. Thus the beam delivered to the calibration chamber has the electric vector primarily in the horizontal direction. The beam polarization measured in the 10-30 nm range is 80% to 90%, and the polarization is expected to be the same at shorter wavelengths.

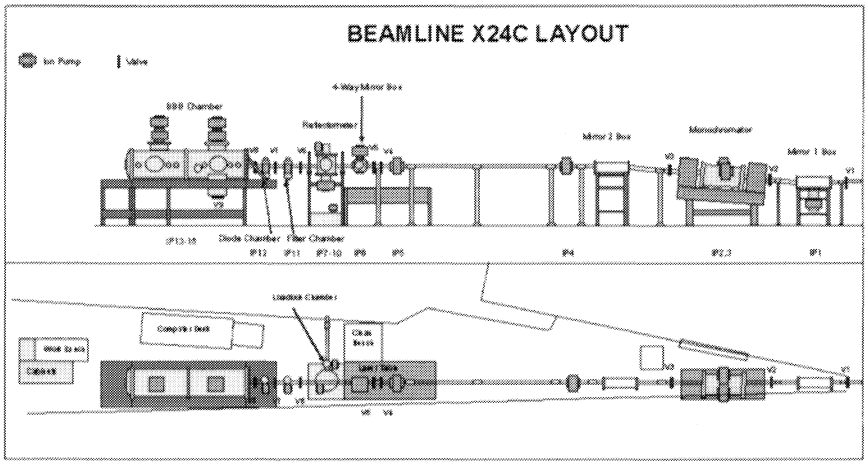

Fig. 1. The NRL beamline X24C and calibration chambers

The grating was mounted in the off-plane orientation as shown schematically in Fig. 2. The grating wafer was mounted by a three-point support onto a goniometer platform with the grooves parallel to the incident radiation. The goniometer platform could be rotated by computer control about two orthogonal axes in the horizontal plane to precisely adjust the incidence angle (θ), with respect to the normal to the grating surface, and the azimuthal angle (ϕ) about the incident radiation beam. The goniometer was mounted on a support plate with x and y motions to accurately position the grating in the radiation beam. The support plate could also be rotated in yaw angle about an axis perpendicular to the goniometer base and at the center of the grating, thereby varying the alignment of the grooves with the incident radiation beam. Finally, the support plate (and goniometer) could be rotated by 90° about the incident radiation beam to the TE (δ=0) or TM (δ=90°) polarization orientations. Thus the grating had four rotational and two translational degrees of freedom.

The conical diffraction pattern was recorded by a phosphor (Gd_2O_2S:Eu) coated CMOS imager with 2" square active area and 48 μm pixels. The CMOS imager was mounted on a support fixture with four computer-controlled motions: x, y, rotation about the vertical axis, and pitch about the horizontal axis. The large area of the CMOS imager provided the ability to capture the entire conical diffraction pattern as shown in Fig. 3. The CMOS imager is controlled by a USB interface to a notebook computer, and the exposure and image download times are typically 10 sec. Thus one can quickly recognize the diffraction features and move to the desired grating angles and incident wavelengths in practically real time.

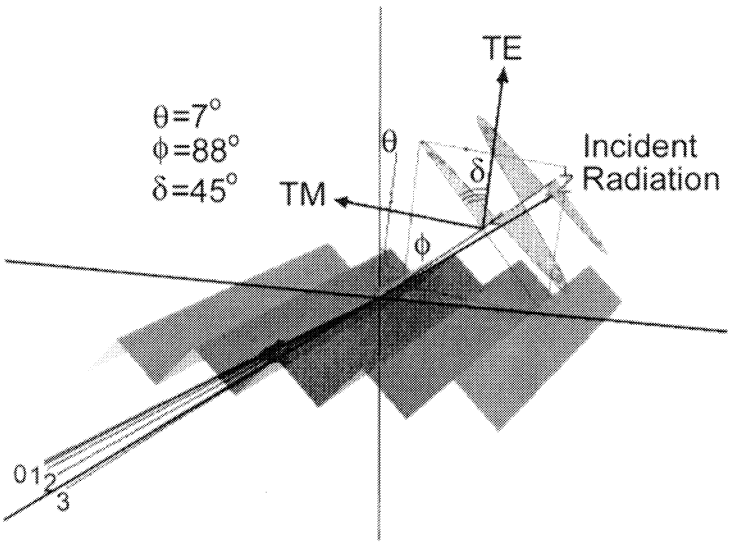

Fig. 2. Schematic of the off-plane grating and the conical diffraction pattern.

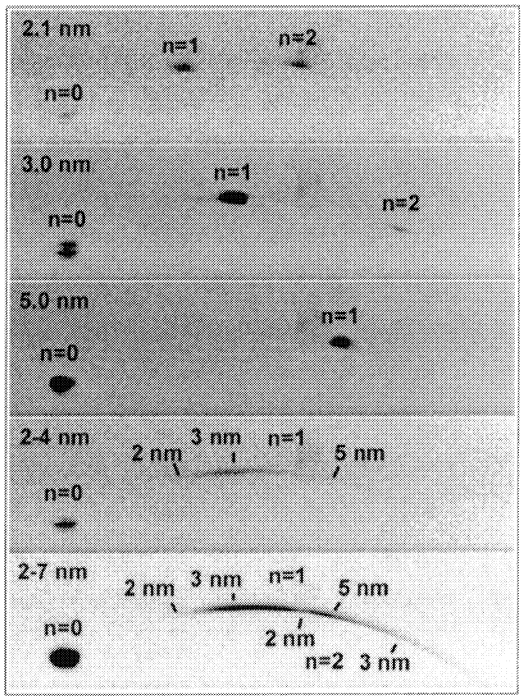

Fig. 3. CMOS images of the conical diffraction pattern for illumination by monochromatic radiation with wavelengths 2.1 nm, 3.0 nm, and 5.0 nm and by broadband radiation 2-4 nm and 2-7 nm.

In most cases, the grating angles were selected to correspond to an off-plane configuration proposed for the *Constellation-X* mission.[7] The grating was positioned at a grazing angle of 1.73°, and the grating was yawed by an angle of 1.0° so the blazed groove facets slightly faced the incident beam. Referring to the grating equation for conical diffraction, $\sin\alpha+\sin\beta=m\lambda/d\sin\gamma$,[17,18,8] under these conditions the cone angle is γ=2.0° and the incidence angle with respect to the grating normal is α=30.0°. The +1 order was closest to being on blaze and appeared near the top (β=0) of

the diffraction cone as illustrated in Fig. 3. The on-blaze condition is that the angles of incidence and diffraction from the grating facets are equal (specular reflection), and then $\alpha+\beta=2\varepsilon$ where ε is the blaze angle.

A 0.5 mm aperture defined the size and position of the beam that was incident on the grating. The aperture insured that the beam illuminated a fixed area on the grating. The 0.5 mm beam underfilled the 5 cm grating grooved area at 1.73° typical grazing angle.

By illuminating the test grating with the zero order of the monochromator gratings and inserting thin metal filters in the beam, it was possible to illuminate the test grating with broadband radiation. Figure 3 shows portions of CMOS images for the case of two broad bands of radiation, provided by the monochromator's filtered zero order, and three discrete wavelengths (2.1 nm, 3.0 nm, and 5.0 nm) dispersed by the monochromator's first order. The lower wavelength limit of the two bandpasses (2 nm) was established by the selected monochromator grazing angle (5.4°). The upper wavelength limits were determined by the beam filtration. Numerous thin metal filters are mounted on two translation vacuum feedthroughs at X24C, and one or two selected filters can be easily moved into the beam. The 2-7 nm bandpass was established by a 158 nm thick aluminum filter (the wavelengths transmitted by the filter longer than the aluminum L edge at 17 nm were dispersed beyond the field of view of the CMOS imager). The 2-4 nm bandpass was established by a 200 nm thick nickel filter in combination with the aluminum filter.

Figure 3 illustrates the ability to easily illuminate the test grating with selected monochromatic radiation or bright broadband radiation. This simulates the two extreme cases when a spectrometer containing the off-plane grating is illuminated by a radiation source with spectral line emission or continuum emission. In addition, when illuminated by monochromatic radiation at the X24C beamline, the absence of continuum dispersed between the orders permits the study of monochromatic radiation scattered from the grating facets. These are critically important measurements for the test gratings which can determine the ability to carry out the science objectives of an astrophysical or solar mission. In contrast, an electron bombarded anode x-ray source provides discrete characteristic x-ray lines and an underlying x-ray bremsstrahlung continuum that is impossible to eliminate. The bremsstrahlung continuum is diffracted between the orders and cannot be distinguished from scattering from the grating facets appearing between the orders. Thus synchrotron measurements provide un-obscured efficiency measurements which are not possible with a laboratory x-ray source.

3. EFFICIENCY MEASUREMENTS

While the CMOS images provided snapshots of the entire conical diffraction pattern and could be used to derive the efficiencies, a more accurate technique is to use absolutely calibrated silicon photodiodes with known linear response over many decades and low noise. The photodiodes were of two types, AXUV-100 with 10x10 mm^2 active area and AXUV-96 with 6x16 mm^2 area, both from International Radiation Detectors Inc. Three photodiodes were mounted on the same support fixture as the CMOS imager and could be moved into the radiation beam under computer control. The three photodiodes had the following apertures: 6.4 mm round (photodiode type AXUV-100), 9.6 mm round (AXUV-100), and 3 mm x 16 mm rectangular (AXUV-96). Based on the positions of the dispersed orders in the CMOS image, a selected photodiode could be accurately moved to the dispersed orders for the measurement of the absolute intensity. An additional photodiode was mounted between the grating and the 0.5 mm aperture for the purpose of measuring the direct beam without having to move the grating from the beam. The beam underfilled all of the photodiode apertures, and the photodiodes were cross calibrated.

Since the zero order beam diffracted from the test grating does not move in angle when the incident wavelength is scanned, it was possible to position a photodiode in the zero order and scan the wavelength in small steps (0.01 nm) while recording the photodiode current at each step. Small wavelength steps are necessary to observe polarization anomalies that were predicted (by PCGRATE-SX calculations[6]) to occur primarily in the TM orientation. The absolute zero order efficiency was derived by dividing by the direct beam current. The resulting zero order efficiency is shown in Fig. 4(Left), and no efficiency jumps resulting from TM polarization anomalies were observed.

The 3 mm x 16 mm aperture was sufficiently tall to intercept a number of diffracted orders near the top of the diffraction cone when scanned horizontally across the diffraction pattern under computer control. The efficiencies in the

dispersed orders were normalized by the measured 0 order efficiency. Shown in Fig. 4(Center) are the 0 and +1 order TM efficiencies when the wavelength was stepped from 3.0 nm to 5.1 nm in 0.1 nm increments. The change in the horizontal position of the +1 order is consistent with the grating equation which predicts a horizontal change by $m\lambda/d$.[1] Shown in Fig. 4(Right) are the 0, +1, and +2 order TM efficiencies measured by positioning the 6.4 mm apertured photodiode in the orders. Small features appear near the K edges of O (2.28 nm) and N (3.10 nm) resulting from slightly different thin films on the surfaces of the two photodiodes used for the measurements (the SiO_2 photodiode surfaces are nitrided for radiation hardness).

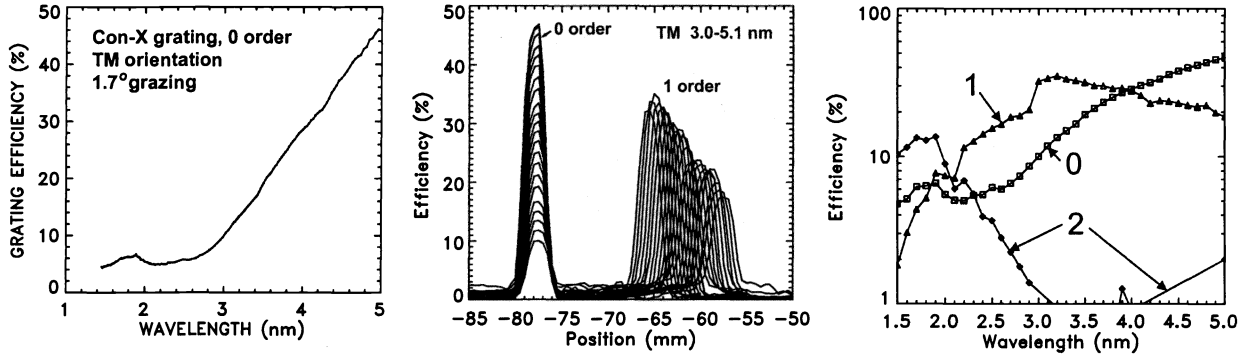

Fig. 4. Left: The measured 0 order TM efficiency. Center: Detector scans through the 0 and +1 orders for 3.0-5.1 nm incident wavelengths. Right: The measured 0, +1, and +2 order efficiencies.

The efficiencies measured in the TE grating orientation, recorded prior to the TM measurements, are not as complete as the TM data because prominent polarization anomalies were not predicted to occur in the TE orientation. In addition, the CMOS imager and the photodiode detectors were positioned closer to the grating during the TE measurements, and this affected the quality of the short wavelength (<3 nm) data where the diffracted orders were not well separated. However, the diffracted orders were well separated at the longer wavelengths (>3 nm), and the measured TE efficiencies in the 0 and +1 orders are shown in Fig. 5 along with the TM efficiencies for comparison. The efficiencies measured in the TE and TM orientation significantly differ, and this indicates that the grating has polarization sensitivity when in the off-plane mount.

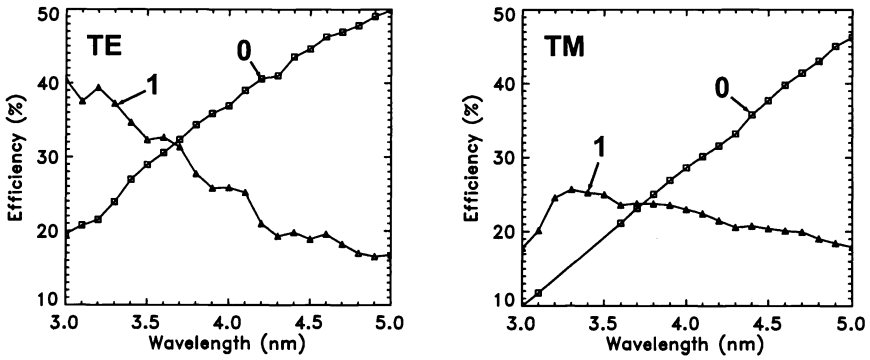

Fig. 5. The measured TE (left) and TM (right) efficiencies in the 3 nm to 5 nm wavelength range.

4. EFFICIENCY CALCULATIONS

The measured TM and TE efficiencies were compared to the efficiencies calculated by the PCGRATE-SX code developed by Goray.[6] For the case of normal incidence gratings with opaque coatings (e.g. gold or aluminum) and multilayer interference coatings, this code has been validated by detailed comparisons to efficiencies measured using

synchrotron radiation (Refs. 19 and 20 and references therein). PCGRATE-SX was recently used to design and fabricate the multilayer coated grating for the Extreme Ultraviolet Imaging Spectrometer (EIS) for the *Solar-B* mission.[20]

Initial comparisons indicated that the efficiencies calculated assuming a 7° blaze angle, the value expected from the grating fabrication process, were in fundamental disagreement with the measured efficiencies. This can be seen by calculating the on-blaze wavelength: $\lambda=2d\sin\varepsilon\sin\sigma$ where the assumed blaze angle is $\varepsilon=7°$ and the grazing angle on the grating facets is $\sigma=1.75°$ (differing slightly from the grazing angle 1.73° with respect to the grating surface). The calculated on-blaze wavelength is $\lambda=1.5$ nm, while the observed TM +1 order efficiency peaks at 3.3 nm (Fig. 4 Right) implying a 15° blaze angle.

An AFM study of the grooved area confirmed the larger than expected blaze angle. The AFM scans across the grooves near the center of the grating are shown in Fig. 6(Left), where each scan is displaced vertically by 1 nm for ease of viewing. The standard deviation of the data points from the average scan curve is 0.89 nm and is a measure of the microroughness of the groove profile. The histogram of the angles between each pair of scan points is shown in Fig. 6(Right), where a Gaussian curve is fitted to the angle distribution. The top corners of the groove profiles are rounded, and this results in a rather broad distribution of angles with a centroid value of 13°. The average values of the blaze angles measured at seven points distributed on the grooved area ranged from 8.9° to 15°, and the microroughness values ranged from 0.66 nm to 0.92 nm. Thus there was considerable variation of the grooves over the 5 cm patterned area. AFM data that were taken before Ti/Au coating of the imprinted grating showed microroughness of approximately 0.2 nm[16] and blaze angles around 8° which indicate that deposition of the metal films onto the polymer-based imprint resist led to the observed changes in groove profile.

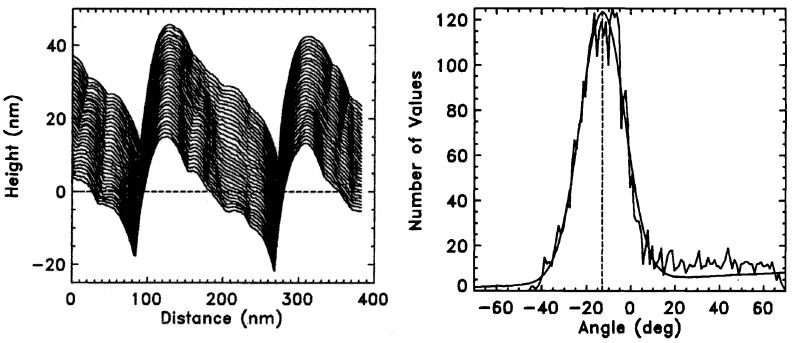

Fig. 6. Left: AFM scans across the grooves. Right: Histogram of the angles of pairs of points on the AFM scans giving a measure of the average blaze angle.

PCGRATE-SX calculations were initially performed using a representative groove profile from the AFM image shown in Fig. 6 and with 1.0 nm microroughness. The incident beam was assumed to be 80% polarized. The efficiencies calculated for the grating in the TE and TM orientations are shown by the solid curves in Fig. 7. A sharp spike (or jump) in efficiency occurs when the diffraction angle of an order, measured from the grating normal, exceeds 90°. Thus as the wavelength increases, efficiency jumps in the lower orders occur when higher orders are diffracted into the grating surface and become evanescent. The efficiency jumps are deeper in the TM orientation where the electric vector of the diffracted wave is approximately parallel to the surface of the grating (see Fig. 2 for $\delta=90°$).

Shown by the dashed curves in Fig. 7 are the measured efficiencies from Fig. 4(Right). As seen in Fig. 7(a), the calculated and measured TE efficiencies are in good overall agreement, except that the small anomalous jumps in efficiency were not observed. Large differences between the calculated and measured TM efficiencies occur in Fig. 7(b), including the absence of the predicted large anomalous jumps in efficiency. The measurement of the TM 0-order efficiency with small wavelength steps (0.01 nm) shown in Fig. 4(Left) conclusively indicates that efficiency jumps are not observed. Other comparisons indicated that the measured TM 2 order, and the measured ratio of the 2 to 1 orders, significantly disagree with the calculations.

There are several possible explanations for the disagreements between the calculated and measured efficiencies. First, the AFM images indicate that the groove profile varies over the grooved area, and the calculated efficiencies differ

significantly when different groove profiles are assumed. Second, the incident beam is not purely (100%) polarized, and this somewhat reduces the ability to observe strong polarization effects in the TM orientation. Finally, the microroughness along the grooves was not measured by AFM scans along the grooves, and incorrect assumed microroughness may affect the calculated efficiencies.

To illustrate the sensitivity of the calculated efficiencies to small changes in the assumed groove profile, Fig. 8 shows the TM efficiencies calculated assuming 36.2 nm groove depth (rather than 24.8 nm depth for the calculations shown in Fig. 7) and 0.5 nm microroughness. Efficiency jumps are absent, and the calculated efficiencies shown in Fig. 8 are in qualitative agreement with the measured TM efficiencies shown in Fig. 4(Right) although the absolute values of the calculated and measured efficiencies differ.

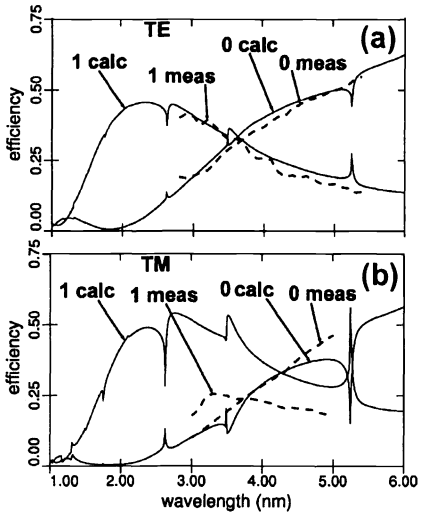

Fig. 7. Calculated (solid curves) and measured (dashed curves) efficiencies in the (a) TE and (b) TM grating orientations.

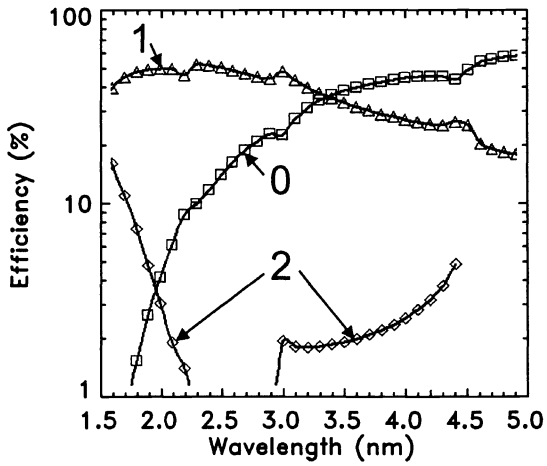

Fig. 8. Calculated TM efficiencies for an assumed groove profile with 36.2 nm depth and 0.5 nm microroughness.

5. DISCUSSION

The absolute efficiency of a 5000 groove/mm grating in the off-plane mount was measured in the TM and TE orientations using polarized synchrotron radiation. The measured efficiencies were compared to the efficiencies calculated using the PCGRATE-SX code. The efficiency jumps predicted by code calculations were not observed, presumably because of the variation of the groove profile over the area illuminated by the grazing incidence radiation beam. The calculated and measured TE absolute efficiency values were in good agreement, while significant differences occurred for the TM values. Further experimental and computational studies are necessary to identify the cause of the TM differences, including detailed AFM characterizations of the shape and microroughness of the groove profile across the grating area. Also the calculation model should be improved to predict TM efficiencies within anomalies more accurately.

For a given wavelength, the measured first-order TE and TM efficiencies differ, and the off-plane grating therefore has polarization sensitivity. This can be exploited to measure the polarization of radiation from astrophysical, solar, and laboratory sources in the soft x-ray region.

This work was supported by the Office of Naval Research and by the National Aeronautics and Space Administration. The National Synchrotron Light Source is operated by the Department of Energy.

6. References

1. W. Cash, "Echelle spectrographs at grazing incidence," Appl. Opt. **21**, 710 (1982).
2. M. C. Hettrick and S. Bowyer, "Variable line-space gratings: new designs for use in grazing incidence spectrometers," Appl. Opt. **22**, 3921 (1983).
3. W. Cash, "X-ray spectrographs using radial groove gratings," Appl. Opt. **22**, 3971 (1983).
4. M. C. Hettrick, "Aberrations of variable line-space gazing incidence gratings in converging light beams," Appl. Opt. **23**, 3221 (1984).
5. W. C. Cash, "X-ray optics. 2: A technique for high resolution spectroscopy," Appl. Opt. **30**, 1749 (1991).
6. L. I. Goray, "Rigorous efficiency calculations for blazed gratings working in in- and off-plane mountings in the 5-50-Å wavelength range," SPIE Proc. 5168, 260 (2004).
7. X-Ray Polarimetry Workshop, SLAC, Stanford CA, 9-11 February 2004), http://www-conf.slac.stanford.edu/xray_polar/Talks.htm.
8. W. Werner, "X-ray efficiencies of blazed gratings in extreme off-plane mountings," App. Opt. **16**, 2078 (1977).
9. M. Neviere, D. Maystre, and W. R. Hunter, "On the use of classical and conical diffraction mountings for xuv gratings," J. Opt. Soc. Am. **68**, 1106 (1978).
10. D. Windt and W. Cash, "Laboratory evaluation of conical diffraction spectrographs," SPIE Proc. 503, 98 (1984).
11. E. Wilkinson, J. C. Green, and W. Cash, "The extreme ultraviolet spectrograph: a radial groove grating, sounding rocket-borne, astrophysical instrument," Ap. J. Suppl. **89**, 211 (1993).
12. R. McEntaffer, S. Osterman, W. Cash, J. Gilchrist, J. Flamand, B. Touzet, F. Bonnemason, and C. Brach, "X-ray performance of gratings in the extreme off-plane mount," SPIE Proc. 5168, 492 (2004).
13. R. McEntaffer, F. Hearty, B. Gleeson, and W. Cash, "An x-ray test facility for diffraction gratings," SPIE Proc. 5168, 499 (2004).
14. R. K. Heilmann, M. Akilian, C.-H. Chang, C. Chen, C. Forest, C. Joo, P. Konkola, J. Montoya, Y. Sun, J. You, and M. L. Schattenburg, "Advances in reflection grating technology for Constellation-X," SPIE Proc. 5168, 271 (2004).
15. A. Rasmussen, A. Aquila, J. Bookbinder, C.-H. Chang, E. Gullikson, R. K. Heilmann, S. Kahn, F. Paerels, and M. L. Schattenburg, "Grating arrays for high-throughput soft x-ray spectrometers," SPIE Proc. 5168, 248 (2004).
16. C.-H. Chang, J. C. Montoya, M. Akilian, A. Lapsa, R. K. Heilmann, M. L. Schattenburg, M. Li, K. A. Flanagan, A. P. Rasmussen, J. F. Seely, J. M. Laming, B. Kjornrattanawanich, and L. I. Goray, "High Fidelity Blazed Grating Replication using Nanoimprint Lithography,", J. Vac. Sci. Technol. B **22**, 3260 (2004).
17. G. Spencer and M. Murty, "General ray-tracing procedure," J. Opt. Soc. Am. **52**, 672 (1962).
18. D. Maystre and R. Petit, "Principe d'un spectromètre à réseau à transmission constante," Opt. Commun. **5**, 35 (1972).
19. L. I. Goray and J. F. Seely, "Efficiencies of master, replica, and multilayer gratings for the soft x-ray - EUV range: modeling based on the modified integral method and comparisons to measurements," Appl. Opt. **41**, 1434 (2002).
20. J. Seely, C. Brown, D. Windt, S. Donguy, and B. Kjornrattanawanich, "Normal-incidence efficiencies of multilayer-coated laminar gratings for the extreme-ultraviolet imaging spectrometer (EIS) on the *Solar-B* mission," Appl. Opt. **43**, 1463 (2004).